ORIGINAL PAPER

Investigating climate change over 1957–2016 in an arid environment with three drought indexes

Behnam Ababaei[1] [ORCID] · Hadi Ramezani Etedali[2]

Abstract

Droughts are typical of the climate in Iran and have become more frequent over the last few decades. Iran's agriculture, water resources, and ecosystems are all vulnerable to drought. In this study, the monthly time series of precipitation, temperature, and potential evapotranspiration were obtained from the CRU TS 4.01 gridded dataset to calculate the Standardized Precipitation Index (SPI), the de Martonne Aridity Index (DMAI), and the Standardized Precipitation-Evapotranspiration Index (SPEI) during two 30-year periods (1957–1986 and 1987–2016). At the national scale, the annual SPI, DMAI, and SPEI have decreased by 0.02, 0.11, and 0.09 unit decade^{-1}, respectively, since the beginning of the twentieth century. Over 1987–2016, these rates increased to 0.29, 0.70, and 0.36 unit decade^{-1}. Over the period 1957–1986, 89.5% of the total area was classified by the DMAI as hyper-arid, arid, or semi-arid, increasing to 94.8% over 1987–2016. Over the period 1987–2016, around 42.1, 57.9, and 48.8% of the grid cells revealed significant ($P < 0.1$) decreasing trends in the annual SPI, DMAI, and SPEI, respectively (27.1, 45.5, and 35.6% at the 95% confidence level). Winter has made the largest contribution to the temporal variations of all indexes at the annual scale. Spatiotemporal variations of the SPEI were greater than the two other indexes since it considers the non-stationarity in potential evapotranspiration. It proved to be an appropriate climatic index for investigating the spatiotemporal variations of agricultural drought, as it considers the source and demand terms of the water balance equation. Analysis of the frequency of sever to moderate droughts during the two 30-year periods confirms that country's climate has significantly changed, especially in central, western, southwestern, southern, and eastern regions.

1 Introduction

Droughts are typical of the climate in Iran and have become more frequent over the last few decades (Raziei et al. 2009; Golian et al. 2015). They cause significant economic losses

✉ Behnam Ababaei
  b.ababaei@uq.edu.au

  Hadi Ramezani Etedali
  ramezani@eng.ikiu.ac.ir

[1] Queensland Alliance for Agriculture and Food Innovation (QAAFI), The Centre for Crop Science, The University of Queensland, Toowoomba, QLD 4350, Australia

[2] Department of Water Sciences and Engineering, Imam Khomeini International University, Qazvin, Iran

and affect all aspects of society (Lott and Ross 2005; Mote et al. 2005; Barnett et al. 2008; Fontaine and Steinemann 2009; Elsner et al. 2010; Zhai et al. 2010). Iran's agriculture, water resources, and ecosystems are all vulnerable to drought (Madani 2014). Therefore, it is essential to investigate the spatiotemporal variations of drought at various spatial and temporal scales in order to effectively manage this natural hazard. Drought is often characterized as having low precipitation and high temperature. It is determined based on temporary deviation from long-term averages and indicates climate situation during specific time periods (Shelton 2009; Karamouz et al. 2012).

Increasing greenhouse gases has led to climate change in all regions of the world over recent decades, identified as changes in weather variables such as precipitation, evapotranspiration, and air temperature (IPCC 2013). Therefore, it is important to understand the impacts of temporal variations in weather variables on aridity and drought, especially in arid and semi-arid regions of the world, such as Iran. Aridity and drought are assessed by

a large set of climatic indexes, most of which calculated based on precipitation and/or temperature (Deniz et al. 2011; Karamouz et al. 2012; Tabari and Aghajanloo 2013). The Palmer Drought Severity Index (PDSI; Palmer 1965), the decile index (DI; Gibbs and Maher 1967), the China-Z index (CZI; Wu et al. 2001), the Surface Water Supply Index (SWSI; Shafer and Dezman 1982), the Standardized Precipitation Index (SPI; Mckee et al. 1993), and the Standardized Precipitation-Evapotranspiration Index (SPEI; Vicente-Serrano et al. 2010) are among the well-known drought indexes. The de Martonne Aridity Index (DMAI; Martonne 1920), the Johansson Continentally Index (JC), the Kerner Oceanity Index (KOI), and the Pinna Combinative Index (PV; Baltas 2007; Deniz et al. 2011) are the most popular aridity indexes. The SPI is widely accepted since it only needs precipitation data, is comparable in time and space (Guttman 1998), and can be calculated at different time scales to monitor droughts (Vicente-Serrano et al. 2010). However, the SPI does not account for the variations in other variables that may have influence on water balance and drought, especially temperature and potential evapotranspiration. It is not always justifiable to use a precipitation-based index by assuming that the variability of precipitation is much higher than other weather variables, especially in warm and dry periods of year when temperature and potential evapotranspiration have much larger values and variations.

Many studies have adopted aridity indexes (Hundecha and Bárdossy 2005; Wilks 2006; Baltas 2007; Shelton 2009; Deniz et al. 2011; Rajabi and Shabanlou 2012; Tabari and Aghajanloo 2013; Irannezhad et al. 2014; Zolfaghari et al. 2016; Moral et al. 2017; Araghi et al. 2018) and drought indexes (Robock et al. 2000; Qian et al. 2003; Zou et al. 2005; Morid et al. 2006; Xin et al. 2006; Zhai et al. 2010; Shukla et al. 2011; Wang et al. 2011; Mahajan and Dodamani 2015; Zhang et al. 2015) to investigate spatiotemporal climatic patterns. It requires access to quality, complete time series of weather data to calculate drought and aridity indexes, which are not easily accessible in most developing countries and data-scarce regions of the world. This limitation, especially in large-scale studies, justifies the application of gridded global/regional datasets as promising alternatives to weather station observations. Given the importance of understanding the variations of drought events in time and space especially in arid regions like Iran, the objective of this paper is to investigate the spatiotemporal variations of the DMAI, SPI, and SPEI at the monthly, seasonal, and annual scales using the monthly time series obtained from the CRU TS dataset over the last 60 years. The implications of the observed changes over the last decades are discussed.

2 Materials and methods

2.1 Study area

Iran, with an approximate area of 1.648 m km^2, is located in the Middle East between 25 and 40° N latitude and 44–63° E longitude (Fig. 1). The country's climate is largely influenced by the presence of two mountain ranges, the Alborz in the north and the Zagros along the western borders beginning from the northwest and ending at the Strait of Hormuz in the south, along with two great deserts, Dasht-e Lut and Dasht-e Kavir. The foothills of the two mountain ranges are classified as having Mediterranean climate, though the country is dominantly classified as arid (65%) and semi-arid (20%) (Madani 2014; Khalili et al. 2016).

Cold winters with heavy snowfalls and negative temperatures during December and January and relatively mild springs and autumns are common in the northwest while moderate winters and hot summers are typical of southern and southeastern regions (Saboohi et al. 2012). Precipitation is highly variable in both time and space (Raziei et al. 2012, 2014). Annual precipitation ranges 62–345 mm (250 mm, on average) with around 70% of annual rainfall falling between November and March (Raziei et al. 2005). A narrow strip in the north along the coast of the Caspian Sea has a very different climate where heavy rainfalls start in late summer and continue through to mid-winter, though in general, it receives > 800 mm of rainfall more or less over the whole year (Raziei et al. 2014).

2.2 Data

The CRU TS dataset (Mitchell and Jones 2005; Harris et al. 2014), developed principally by the UK's Natural Environment Research Council (NERC) and the US Department of Energy, is among well-tested and popular publicly available gridded datasets. It covers the global land surface between 60° S and 80° N over 1901–2016 and contains data on 10 weather variables from over 5000 weather stations interpolated into 0.5° × 0.5° grid cells. There proved to be a favorable agreement between the CRU TS dataset and similar gridded datasets, with major deviations attributed to regions with sparse observations (Harris et al. 2014). The accuracy of the CRU TS precipitation data is sufficiently high for hydrological studies in data-scare regions (Hajihoseini et al. 2015). This dataset outperformed the NCEP CFSR gridded reanalysis dataset in the simulation of runoff towards Lake Maharlou in Iran using the Soil and Water Assessment Tool (SWAT) model (Eini et al. 2018). Miri et al. (2016) compared the CRU TS temperature data with data from 88 selected weather stations across Iran and concluded that the CRU TS data explain 95% of the variations in the observed time series.
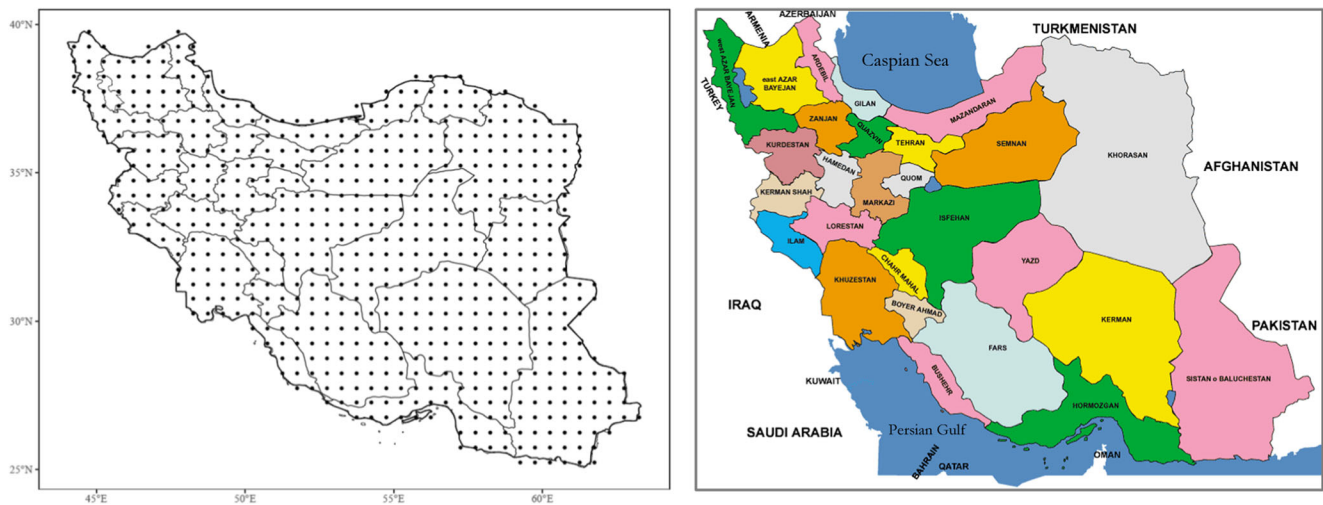
Fig. 1 Selected grid cells from the CRU dataset (left) and administrative divisions of Iran (right)

Monthly average daily mean temperature and potential evapotranspiration (PET) and monthly total precipitation were obtained from the 4.01 release of the CRU TS dataset[1] in 675 grid cells within the country's borders. Potential evapotranspiration in the CRU TS dataset is calculated using a variant of the Penman–Monteith formula (Pereira et al. 2015). Monthly temperature and precipitation data from the CRU TS dataset were compared with observed data from 19 selected stations across the country. The evaluation results are presented in Supplementary Material (Fig. S1–S4) and confirm the acceptable accuracy of the dataset for trend analysis across most parts of the country.

2.3 Aridity and drought indexes

2.3.1 The standardized precipitation index

To calculate the SPI, a probability distribution (here, a gamma distribution) is fitted on a long-term precipitation time series, which is then transformed into a normal distribution so that the mean value is zero (Mckee et al. 1993). Positive/negative values indicate larger/smaller than mean precipitation. The SPI may be used for monitoring both dry and wet conditions (Table 1) and may be computed at different time scales. Here, the SPI is calculated at annual, seasonal, and monthly scales.

2.3.2 The standardized precipitation-evapotranspiration index

The SPEI can be calculated over a wide range of climates and enables comparison of drought severity through time and space. However, a crucial advantage of the SPEI over other widely used drought indexes is that it accounts for the impact of the potential evapotranspiration on drought severity. The SPEI is defined as the difference between precipitation and the potential evapotranspiration at each period (i.e., a month, season, or year) providing a simple measure of the water surplus or deficit (Vicente-Serrano et al. 2010). The SPEI is standardized by fitting a log-logistic distribution on the time series of the differences between precipitation and the potential evapotranspiration. It can therefore be compared with other SPEI values over time and space. The SPEI can be calculated and aggregated at various time scales, following the same procedure as for the SPI (Table 1). The R package "SPEI" version 1.7 was adopted to calculate the SPI and SPEI at various time scales.

2.3.3 De Martonne Aridity Index

The DMAI (Martonne 1920) is one of the oldest aridity/ humidity indexes and is used worldwide for climate classification. To identify the climate based on the DMAI, the classes presented in Table 1 can be employed (Baltas 2007; Araghi et al. 2018). The significance of the change in the 30-year averages of the DMAI in all grid cells was evaluated using the t test at the 90% confidence level.

2.4 Trend analysis

The spatiotemporal variations in the selected indexes were investigated over two 30-year periods, i.e., 1957–1986 and 1987–2016. The significance of temporal trends was assessed using a modified version of the Mann–Kendall (MK) test, which is a rank-based nonparametric test (Kendall and Gibbons 1990; Azim et al. 2018). The calculation procedure of the MK test can be found in many references (e.g., Ahmadi et al. 2018). Trend magnitudes

---

[1] Obtained in June 2018 from: http://data.ceda.ac.uk/badc/cru/data/cru_ts_4.01/data

Table 1 Classification of aridity and drought indexes

Climate type	Ranges of DMAI	Climate type	Ranges of SPI and SPEI
Hyper-arid (HA)*	< 5	Extreme drought (ED)*	SPI, SPEI < − 2.0
Arid (A)*	$5 \leq \text{DMAI} < 10$	Severe drought (SD)*	$-2 \leq \text{SPI, SPEI} < -1.5$
Semi-arid (SA)	$10 \leq \text{DMAI} < 20$	Moderate drought (MD)*	$-1.5 \leq \text{SPI, SPEI} < -1.0$
Mediterranean (M)	$20 \leq \text{DMAI} < 24$	Mild drought (MiD)	$-1.0 \leq \text{SPI, SPEI} < -0.5$
Semi-humid (SH)	$24 \leq \text{DMAI} < 28$	Near normal (NN)	$-0.5 \leq \text{SPI, SPEI} < 0.5$
Humid (H)	$28 \leq \text{DMAI} < 35$	Mildly wet (MiW)	$0.5 \leq \text{SPI, SPEI} < 1.0$
Very humid (VH)	$35 \leq \text{DMAI} < 55$	Moderately wet (MW)	$1.0 \leq \text{SPI, SPEI} < 1.5$
Extremely humid (EH)	> 55	Severely wet (SW)	$1.5 \leq \text{SPI, SPEI} < 2.0$
		Extremely wet (EW)	$2.0 < \text{SPI, SPEI}$

*Moderate to severe (M–S) droughts

(i.e., slope) were estimated with the Theil–Sen approach and the Trend-Free Pre-whitening (TFPW) procedure was applied to remove the effect of serial correlation (Yue et al. 2002). The R package "zyp" was used to carry out the test (Bronaugh and Werner 2015). Grid cells with insignificant trends at a 90% confidence level are shown in gray on the maps.

3 Results and discussion

3.1 Climate classification

Climate classification was performed using the long-term averages of the DMAI over each 30-year period. At the annual scale and over the period 1957–1986 (Fig. 2, Fig. S5), 89.5% of the total area was classified as hyper-arid, arid, or semi-arid, increasing to 94.8% over the period 1987–2016. Mediterranean and semi-humid climates can only be observed in the northwest, north, and along the Zagros mountain ranges, stretching from northwest to southeast. Six grid cells (< 1% of the country's total area) along the shores of the Caspian Sea, the most humid part of Iran, are much drier compared to the

classification performed by Araghi et al. (Araghi et al. 2018) who used the Global Precipitation Climatology Centre (GPCC) dataset (e.g., the Anzali station in Fig. S2). The same deviation was also observed by Miri et al. (2016) across the coastal regions in the north and south, which might stem from the fact that the interpolation algorithm may not be robust in regions where neighboring grid cells have very different climates and/or when insufficient data is available in the surrounding grid cells. No grid cells experienced a significant increase in the DMAI values while grid cells in the northwest, northeast, and southeast experienced significant decreases ($P < 0.10$) over the last three decades as compared with the previous 30-year period.

At the seasonal scale, the spatial pattern of the DMAI in winter follows the main topographic features of Iran (Fig. S6). The Alborz and Zagros mountain ranges have a key role in spatiotemporal variations of temperature and precipitation in the country by blocking moisture flux from the north and west towards the central regions (Tabari and Aghajanloo 2013; Raziei et al. 2014; Araghi et al. 2018). In spring and summer, most of the grid cells are classified as semi-arid, arid, or hyper-arid (Fig. S5). While summer and autumn have the least number of grid
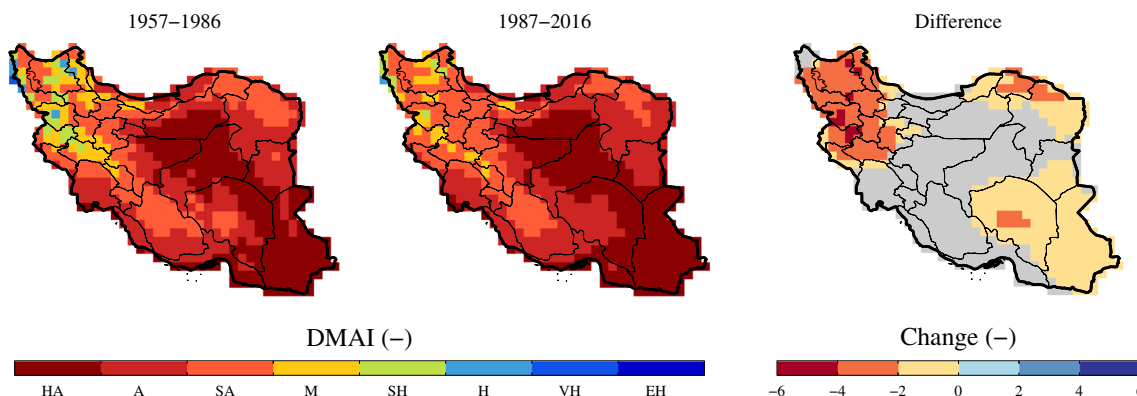

Fig. 2 Climate classification at the annual scale using the DMAI over the 30-year periods of 1957–1986 and 1987–2016. Right panel shows the subtraction of the values averaged over 1987–2016 from the values averaged over 1957–1986. Grid cells with insignificant differences ($P > 0.1$ in the t test) are shown in gray

cells showing significant changes in the DMAI, grid cells in the northwest, northeast, and southeast reveal significant changes as compared with 1957–1986 in winter and spring. In winter, around 47% of the total area are classified as semi-arid, arid, or hyper-arid over 1987–2016, up from 41.4% over the previous 30-year period. The cumulative portion of the grid cells identified as semi-humid, humid, very humid, or extremely humid in winter and spring reduced from 48.7 and 6.7% over 1957–1986 to 43.3 and 1.8% over 1987–2016, respectively.

3.2 Spatiotemporal variations of the SPI

The annual SPI has increased in the central Iran over 1957–1986 at a national average rate of $+0.23$ units decade^{-1} (Fig. 3). However, in the last 30-year period (1987–2016), the annual SPI experienced decreasing trends in the south and east and declined at a national average rate of -0.29 units decade^{-1}. The northern and northwestern provinces experienced no significant trend in the annual SPI over the last 30 years.

Regarding the seasonal SPI, significantly more grid cells experienced decreasing trends in winter than in other seasons (Fig. 4). Over 1957–1986, increasing trends were detected in winter in the central and northeastern provinces while most provinces experienced decreasing trends over the recent 30-year period. As winter is the most humid season in Iran, spatiotemporal trends in the annual SPI is mostly affected by trends of the SPI in winter. Drought in winter has deep negative impact on Iran's water resources, as rainfed agriculture and domestic supply are largely dependent on winter precipitation. Hence, the decreasing trends in the SPI (i.e., precipitation) in winter have significantly decreased rainfed production (Ramezani Etedali et al. 2013). Decreasing trends in the monthly SPI over the second period were detected in

January to March and increasing trends in November (Fig. S7). In other months, most grid cells did not reveal significant trends over the period 1987–2016.

3.3 Spatiotemporal variations of the DMAI

Temporal trends in the annual DMAI over the two periods are presented in Fig. 5. The spatial pattern is very similar to that of the annual SPI. However, as the equations of these two indexes are different, the trends have different magnitudes. This similarity shows that precipitation is a more influential factor on drought than temperature. Like the SPI, the DMAI increased across the central regions of Iran over the period 1957–1986 and decreased in the southwest, south, and east over 1987–2016 at a national average rate of -0.7 unit decade^{-1}. The national average decreasing rate of the DMAI was estimated at -0.11 unit decade^{-1} since 1901, increasing to $+0.61$ unit decade^{-1} over 1957–1986. The spatiotemporal pattern of the DMAI observed in this study is similar to the pattern of the annual DMAI presented by Araghi et al. (2018). Investigating the spatiotemporal pattern of aridity across Iran over 1954–2013, they used two gridded data sets, GPCC v7 and a temperature dataset distributed by the Department of Geography, University of Delaware (hereinafter UD) v4.01.

At the seasonal and monthly scales (Fig. 6, Fig. S8), observed patterns over the period 1987–2016 are more or less similar to those of the SPI. Over this period, most grid cells experienced significant decreasing trends in winter though the grid cells located in the center, west, southwest, and east revealed significant increasing trends over 1957–1986. November is the only month when part of Iran experienced increasing trends in the DMAI over the period 1987–2016.
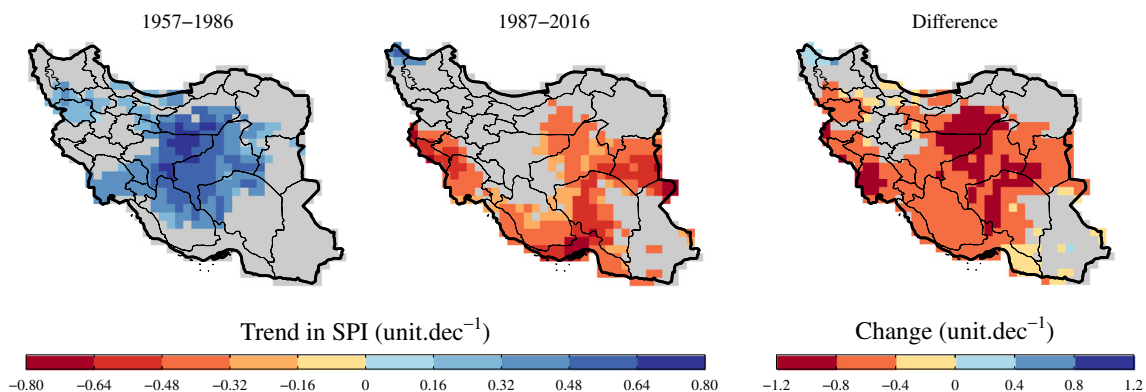

Fig. 3 Temporal trends in annual SPI over 1957–1986 and 1987–2016. Grid cells shown in gray revealed insignificant trends ($P > 0.1$), determined with a modified version of the Mann–Kendall test. Right panel shows the subtraction of the trends over 1987–2016 from the trends over 1957–1986. Differences between the two periods are only shown for grid cells where at least one period experienced a significant trend
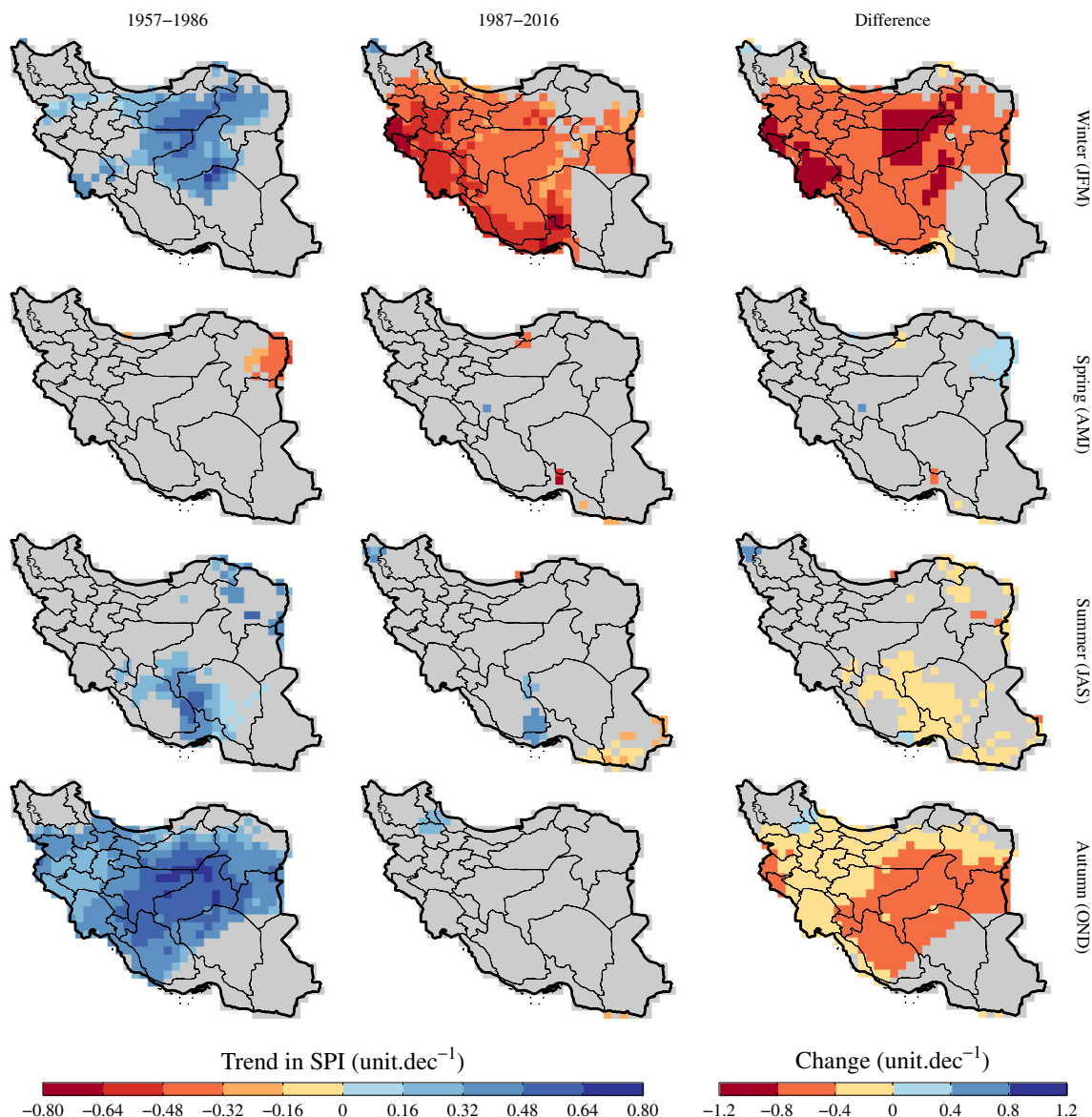
Fig. 4 Temporal trends in seasonal SPI over 1957–1986 and 1987–2016. Grid cells shown in gray revealed insignificant trends (P > 0.1), determined with a modified version of the Mann–Kendall test. Right panel shows the subtraction of the trends over 1987–2016 from the trends over 1957–1986. Differences between the two periods are only shown for grid cells where at least one period experienced a significant trend

3.4 Spatiotemporal variations of the SPEI

The spatiotemporal patterns of the annual SPEI over the two periods are presented in Fig. 7. The SPEI has decreased at a national average rate of -0.09 units decade^{-1} since the beginning of the twentieth century (Fig. 6). This decreasing rate increased to -0.36 unit decade^{-1} over the last three decades. All grid cells in the southwest, south, southeast, and east experienced decreasing trends (mostly between -0.4 and -0.6 unit decade^{-1}) over the period 1987–2016.

At the seasonal scale (Fig. 8), winter, summer, and spring have respectively the largest numbers of grid cells with significant decreasing trends over 1987–2016 while only in autumn some grid cells reveal significant

increasing trends in the SPEI. This stands in contrast to the pattern observed during the period 1957–1986 in which the SPEI increased in > 50% of grid cells in winter and autumn and decreased mostly in the southeast in spring and summer. March (vs November) has the largest number of grid cells revealing significant decreasing (vs increasing) trends of the magnitudes as large as 0.8–1.0 unit decade^{-1}. In January, February, June, July, and August, a large number of grid cells experienced decreasing trends in the SPEI.

3.5 Comparison of three indexes

At the national scale, the SPI has decreased at a rate of -0.02 unit decade^{-1} since 1901 while the rates of decrease in
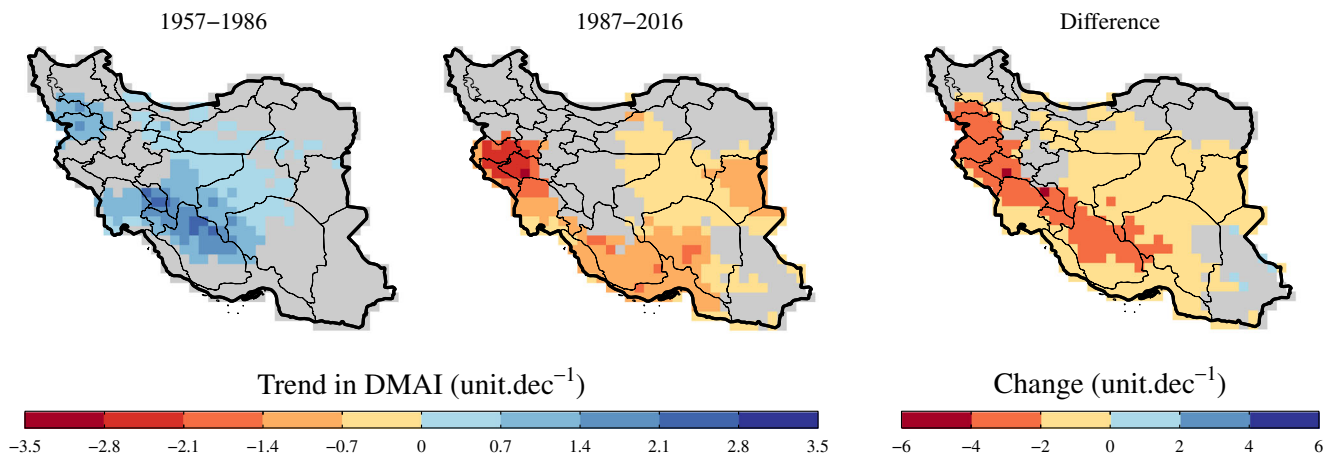
Fig. 5 Temporal trends in annual DMAI over 1957–1986 and 1987–2016. Grid cells shown in gray revealed insignificant trends (P > 0.1), determined with a modified version of the Mann–Kendall test. Right panel shows the subtraction of the trends over 1987–2016 from the trends over 1957–1986. Differences between the two periods are only shown for grid cells where at least one period experienced a significant trend

the DMAI and SPEI were estimated at -0.11 and -0.09 unit decade^{-1}, respectively (Fig. S10). In the calculation of the SPI, only precipitation is taken into account while the DMAI also considers temperature and the SPEI accounts for the potential evapotranspiration as well. The authors have shown (Ramezani Etedali et al. 2018) that over the period 1987–2016, temperature has increased in most of the grid cells across Iran, at a national average rate of 0.39 °C decade^{-1}, for which the DMAI experienced stronger decreasing trend than the SPI. The potential evapotranspiration has increased at a national average rate of 5.64 mm decade^{-1} since 1901 (data not shown), which along with the observed decreasing trends in precipitation (i.e., the SPI) has led the SPEI to experience stronger decreasing trends than the SPI. Since 1987, the SPI, DMAI, and SPEI have decreased at national average rates of -0.29, -0.69, and -0.36 unit decade^{-1}, respectively (Fig. S10).

At the annual scale and over the period 1987–2016, the SPI and DMAI both revealed a significant drying pattern in the west, southwest, south, and central–east while the SPEI also showed the same pattern in the southeast and more grid cells in the center. According to the SPI, a few grid cells in the far northwest experienced increasing trends in the annual SPI (Fig. 3) while no such trends were observed in the time series of the DMAI (Fig. 5) and SPEI (Fig. 7). Both the SPI and DMAI revealed significant decreasing trends in winter in most grid cells and detected no large area experiencing decreasing trends in other seasons. Nonetheless, the SPEI detected large areas with significant decreasing trends in the southeast in spring and in the southeast, east, and central–north in the summer. It must be noted that the SPI is unable to detect trends in grid cells where precipitation does not occur over a specific period or where the climate is classified as hyper-arid with small amount of precipitation falling at the monthly or seasonal scales. The SPEI does not suffer from the same issue as

even with zero precipitation it can detect climatic trends in water deficit/surplus.

In winter, most of the grid cells experienced significant decreasing trends with 2–3 indexes confirming the pattern (Fig. S11). In other seasons, mostly < 2 indexes revealed decreasing trends with the SPEI being one of the two at most grid cells. Autumn has the least number of grid cells with significant trends followed by spring and summer. Over the period 1987–2016, around 42.1, 57.9, and 48.8% of the grid cells revealed significant (P < 0.1) decreasing trends in the annual SPI, DMAI, and SPEI, respectively (27.1, 45.5, and 35.6% at the 95% confidence level; Fig. 9). The largest differences between the SPI and the other two indexes are observed in winter with the former showing that around 61% of the grid cells have experienced significant decreasing trends (P < 0.1) while according to the DMAI and SPEI that portion was estimated at 77.8 and 75.6%, respectively (48.6, 65.8, and 69.3% at the 95% confidence level, respectively).

The frequency of moderate to severe (M–S) droughts (Table 1) has increased in most grid cells over the last three decades as compared with the previous 30-year period (Fig. 10). The patterns of the SPI and SPEI were similar in winter and spring, while the DMAI showed smaller number of grid cells with considerable positive shifts in the frequency of M–S droughts. Most of the grid cells in the northeast experienced a decrease or negligible increase in the frequency of M–S droughts in winter. In spring, most of the grid cells in the southeast did not experience significant changes according to the DMAI or revealed negative shifts according to the SPI and SPEI. While the SPI and DMAI show that the frequency of M–S droughts did not change significantly in many grid cells, most grid cells in the south, center, east, and northeast experienced significant increases according to the SPEI, compared with the period 1957–1986. Since 1957, the national frequency of M–S droughts have increased at the rates of 0.65 (P =

0.591), 0.88 ($P = 0.081$), and 2.26 ($P = 0.136$) % decade^{-1}, according to the annual SPI, DMAI, and SPEI, with the fastest increases observed in spring (1.51 ($P = 0.450$), 2.47 ($P = 0.005$), and 3.18 ($P = 0.132$) % decade^{-1}).

Over the period 1987–2016 and at the annual scale, nearly 38, 28.5, and 58.6% of the grid cells experienced > 10% increases in the frequency of M–S droughts according to the SPI, DMAI, and SPEI, respectively, as compared with the period 1957–1986 (Fig. 11). In all seasons except winter, the SPEI shows more grid cells with significantly more frequent M–S droughts than the other two indexes. In winter, the SPI shows that more than 45.3% of the grid cells experienced > 10% increase in the frequency of M–S droughts, while the SPEI led to a smaller number, 35.9%, due to the smallest

values of the potential evapotranspiration in winter with negligible contribution to the trends of the SPEI as compared with precipitation.

3.6 Data quality and sources of error

3.6.1 CRU TS data quality

Calculation of the selected drought indexes requires complete long-term weather data. Previous studies confirmed that the CRU TS gridded dataset offers quality data in Iran, especially for trend analysis (Hajihoseini et al. 2015; Miri et al. 2016; Eini et al. 2018; Ramezani Etedali et al. 2018). The most comprehensive comparison of the CRU TS dataset with other
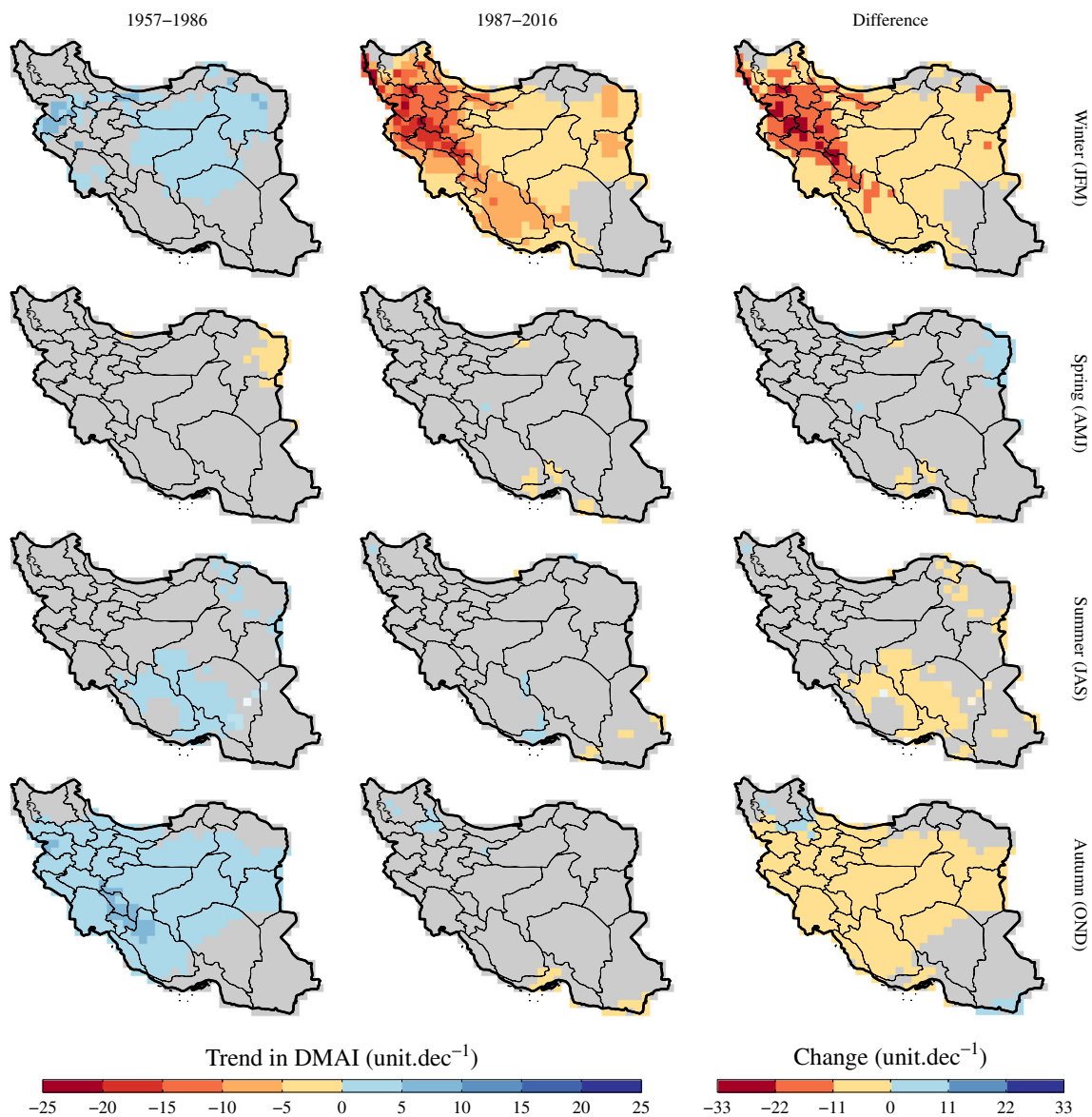

Fig. 6 Temporal trends in seasonal DMAI over 1957–1986 and 1987–2016. Grid cells shown in gray revealed insignificant trends ($P > 0.1$), determined with the Mann–Kendall test. Right panel shows the subtraction of the trends over 1987–2016 from the trends over 1957–1986. Differences between the two periods are only shown for grid cells where at least one period experienced a significant trend
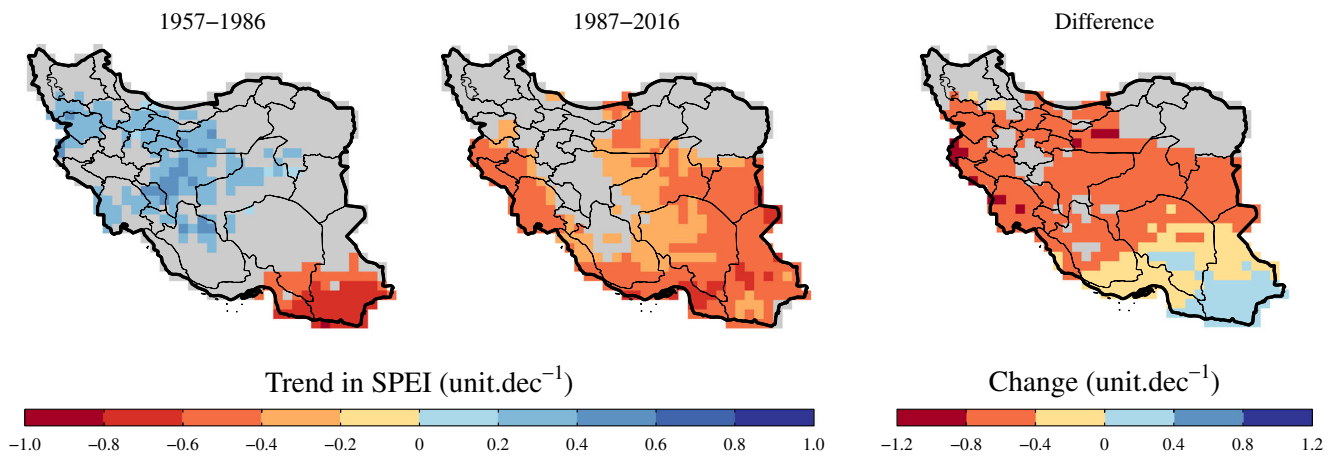
Fig. 7 Temporal trends in annual SPEI over 1957–1986 and 1987–2016. Grid cells shown in gray revealed insignificant trends ($P > 0.1$), determined with the Mann–Kendall test. Right panel shows the subtraction of the trends over 1987–2016 from the trends over 1957–1986. Differences between the two periods are only shown for grid cells where at least one period experienced a significant trend

similar products was carried out by Harris et al. (2014). Adopting the regions introduced by Giorgi and Francisco (2000), they compared the CRU TS dataset (version 3.10) with the temperature dataset developed by the University of Delaware (UDEL) and the 5th version of the precipitation dataset developed by the GPCC v5. The northern half of Iran was assigned to the subcontinental region "Southern Asia." There proved to be good agreements between the CRU TS and the other two gridded datasets with correlations estimated at 0.96 for temperature (over 1901–2008), and 0.53 and 0.91 for precipitation (over 1901–2009 and 1951–2009, respectively). As the number of stations in the GPCC v5 dataset is considerably higher than the CRU TS dataset, these results imply that the CRU TS precipitation data should be treated cautiously over the first half of the twentieth century.

The temporal variations in the CRU TS monthly temperature and precipitation data were compared against data from 19 selected stations across Iran (Fig. S4). While at a number of the selected stations, the CRU TS precipitation data outperformed the data from the GPCC v5 dataset (e.g., Tehran in the center and Bushehr in the southwest, see Araghi et al. 2018), at most of the stations, the latter showed a better agreement with the observed series. Besides the northern coastal regions of the country (Fig. S1–S4), the CRU TS precipitation data showed weak correlations with the observed data in the far northeastern regions, i.e., the area close to the Iran–Afghanistan border where the density of monitoring stations is considerably lower than the other parts of the country (Fig. S1, see the station Mashhad in Fig. S2). Considering that the Correlation Decay Distances (CDDs) were set at 450 mm for precipitation (New et al. 2000; Harris et al. 2014), it has resulted in fewer stations (i.e., lower "station influences") contributing to the interpolation process in grid cells located in this area. Moreover, the trends in the CRU TS temperature data over the "pre-1987" period were underestimated in

nearly 30% of the stations (Fig. S4). Therefore, it can be concluded that the CRU TS dataset is a more reliable source of data for temperature than precipitation over the study area, especially since the 1980s and over the northern and northeastern regions.

3.6.2 Potential evapotranspiration and wind speed

The SPEI is the only index that considers PET along with precipitation. PET is calculated using a variant of the Penman–Monteith method from absolute values of temperature, vapor pressure, and cloud cover in each grid cell and a fixed monthly climatology of wind speed (New et al. 1999; Harris et al. 2014). Many studies reported significant impact of wind speed on PET (e.g., Rana and Katerji 1998; Parsafar et al. 2012; Yang and Yang 2012; Ahmadi et al. 2016). Therefore, adoption of fixed monthly climatology of wind speed could be a source of error if significant changes occur in the wind speed series over time. Ghahraman and Gharakhani (2010) investigated wind speed data at 40 synoptic stations across Iran over the period 1975–2005. At the annual scale, 27.5–40% and 22.5–30% of the studied stations (depending on the statistical test used) experienced "significant" increasing and decreasing trends, respectively. Out of 40 stations, increasing trends were detected in 75% of the stations. Increasing trends were most common in winter and least common in summer while decreasing trends were mostly detected in autumn. Rahimzadeh and Pedram (2011) detected significant decreasing trends in annual average wind speed in Esfahan and Kashan (in the center of Iran) over the period 1961–2005. They concluded that urbanization could explain part of the observed variations. Rezayi Banafsheh et al. (2011) analyzed the wind speed data from seven synoptic stations in northwestern Iran over 1961–2005 and detected significant decreasing and increasing trends in
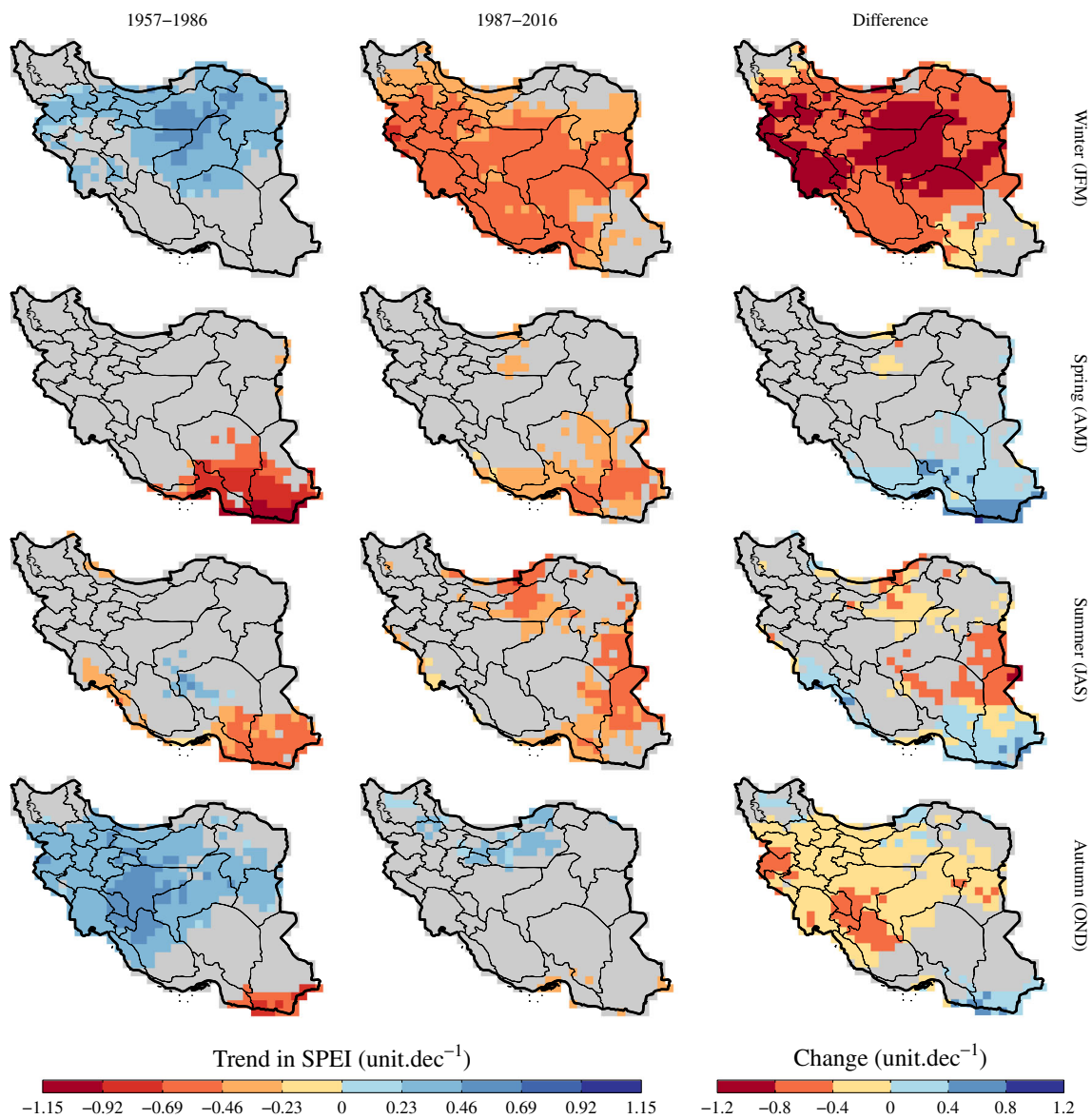
Fig. 8 Temporal trends in seasonal SPEI over 1957–1986 and 1987–2016. Grid cells shown in gray revealed insignificant trends (*P* > 0.1), determined with the Mann–Kendall test. Right panel shows the subtraction of the trends over 1987–2016 from the trends over 1957–1986. Differences between the two periods are only shown for grid cells where at least one period experienced a significant trend

annual average wind speed in two stations, respectively. The same pattern was detected for spring and autumn while the number of stations with significant decreasing and increasing trends were three/one for summer and zero/one for winter. No clear spatial pattern was observed in temporal trends. Afshari Azad and Shabanzadeh (2010) analyzed temporal variations in the wind speed data in Rasht (in the north of Iran) and showed a significant decreasing trend in the annual average wind speed over 1977–2009. However, at the monthly scale, no significant trend was detected in January, September, and November (i.e., autumn and early winter) while increasing trends were detected in February and March (i.e., mid-late winter). Dinpazhooh (2010) revealed significant increasing trends in the monthly average PET in all calendar months in

Zabol (in the southeast of Iran), with trends in June and February being the weakest and strongest, respectively. These trends were mostly attributed to the increased wind speed in the study area. Ahmadi et al. (2016) analyzed the weather data from 12 weather stations in northeastern Iran over 1986–2005 and detected a combination of increasing and decreasing trends in temperature, relative humidity, wind speed, solar radiation, and PET. Detecting decreasing trends in wind speed at 9 out of 12 stations, they concluded that the increasing trends in annual total PET was mostly attributed to the increase in temperature and solar radiation and, to smaller extent, reduced relative humidity. Since the sensitivity of the Penman–Monteith model to variations in wind speed depends on the absolute values of other weather variables, especially
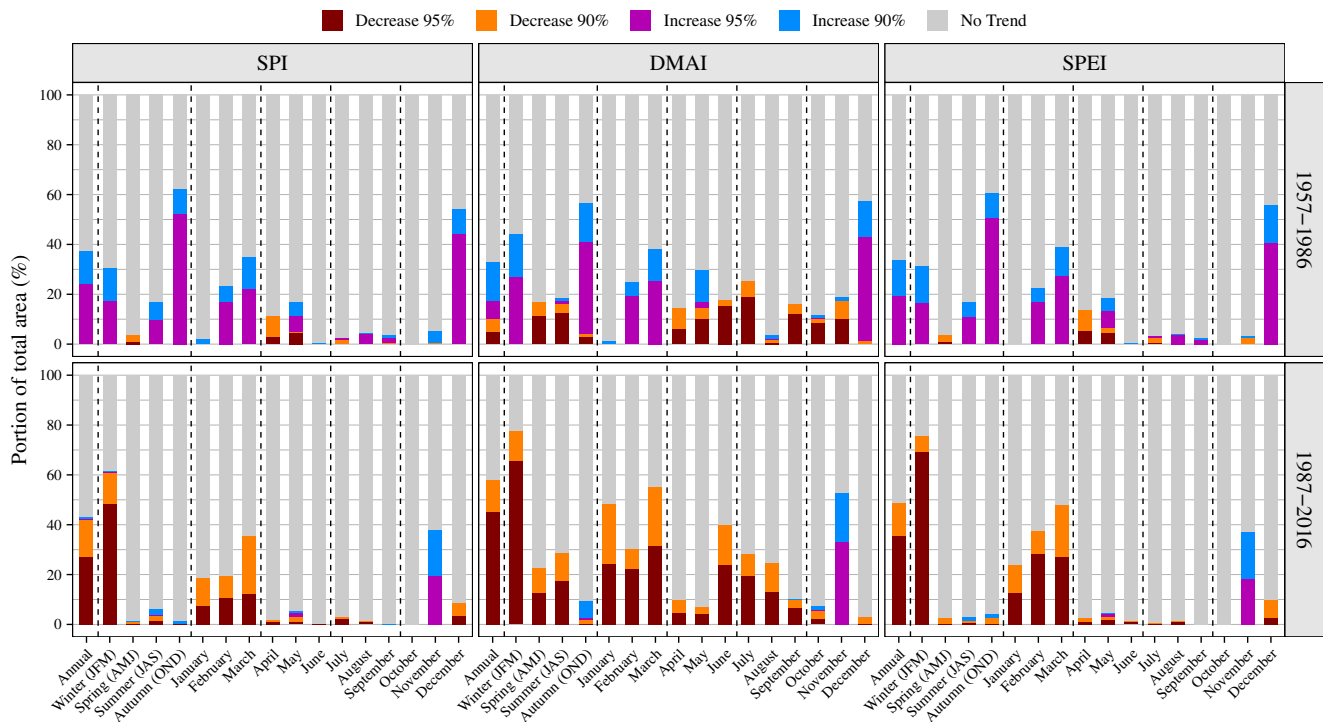
Fig. 9 The portion of the grid cells (i.e., Iran's total area) where significant trends were detected in the annual, seasonal, and monthly time series of the SPI, DMAI, and SPEI at two confidence levels of 90 and 95%

temperature and radiation (Allen et al. 1998; Rana and Katerji 1998; Parsafar et al. 2012), it is not possible to make a general conclusion for the whole country regarding the implications of using fixed monthly wind speeds in the calculation of PET in the CRU TS dataset. However, as increasing trends in wind speed have been mostly reported in different regions of Iran, it is safe to assume that the estimated trends in the SPEI values are relatively conservative in most parts of the country. Nevertheless, it is important to note that in regions with significant decreasing trends in wind speed, the results should be treated with caution.

4 Conclusion

Iran's agriculture and water resources are significantly vulnerable to drought (Madani 2014). Drought has different definitions in climatology, hydrology, agriculture, economy, and social studies (Raziei et al. 2009; Golian et al. 2015). Therefore, three drought indexes including the SPI, SPEI, and DMAI were used to investigate the spatiotemporal variations of drought at various temporal scales in Iran.

Two 30-year periods (1957–1986 and 1987–2016) were compared in terms of spatial patterns and temporal trends. Decreasing (i.e., drying and/or warming) trends of all three indexes in most parts of Iran are the most important finding of this study. However, decreasing trends of

the DMAI and SPEI were stronger than the SPI. The reason is that in the calculation of the SPI, only precipitation is taken into account while the DMAI also considers temperature and the SPEI accounts for the potential evapotranspiration as well. Over the period 1987–2016, the SPI, DMAI, and SPEI have decreased at national rates of -0.29, -0.69, and -0.36 unit decade^{-1}, respectively. The results show that the SPEI is more applicable than the SPI for exploring climate change and drought, especially in agriculture, as concluded in other studies (e.g., Vicente-Serrano et al. 2010; Tan et al. 2015).

Analysis of temporal variations of all three indexes showed that in winter, droughts have become more frequent, more than any other season. Reduced precipitation and increased temperature and potential evapotranspiration in winter, especially in March, have been reported in other studies in Iran (Raziei et al. 2005; Tabari and Hosseinzadeh Talaee 2011; Tabari et al. 2012; Hosseinzadeh Talaee et al. 2013; Tabari and Aghajanloo 2013; Ghasemi 2015; Gu and Adler 2015; Bazrafshan 2017; Davy et al. 2017). Winter precipitation and snowfall have a critical role in the supply of surface water resources in Iran. Reduction in precipitation and more frequent droughts in winter can significantly reduce the reserved volume of dams, which are essential sources of domestic and agricultural water in spring and summer. It puts more pressure on already scarce and unstable ground water resources of the country, which are already confirmed to have dropped below a critical level
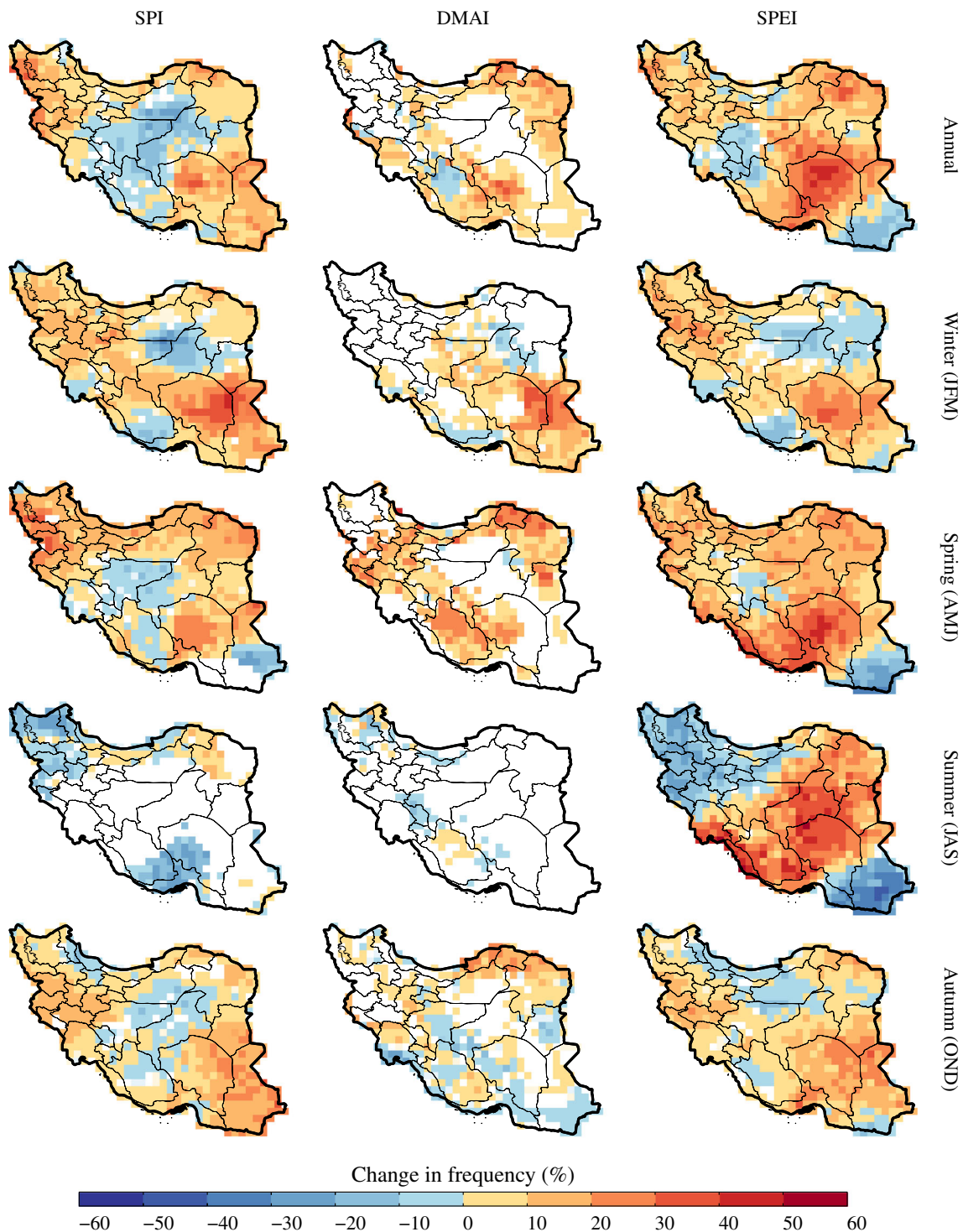
Fig. 10 Change in the frequency of moderate to severe (M–S) droughts over 1987–2016 as compared with the period 1957–1986, according to the SPI, DMAI, and SPEI. Grid cells shown in white did not experience any change or no M–S drought was recorded in one or both of the two periods. For the thresholds used to define M–S droughts, please refer to Table 1

in most plains in Iran, especially in regions where intensive agriculture is practiced (Mojtabavi et al. 2018).

Reduced precipitation and more frequent drought in winter could have adverse impact on rainfed winter crops.

Winter precipitation is the main source of water to meet the requirements of wheat, barley, and colza, especially during grain filling period (Ababaei et al. 2014; Ramezani Etedali et al. 2016). Hence, given the observed reduction in
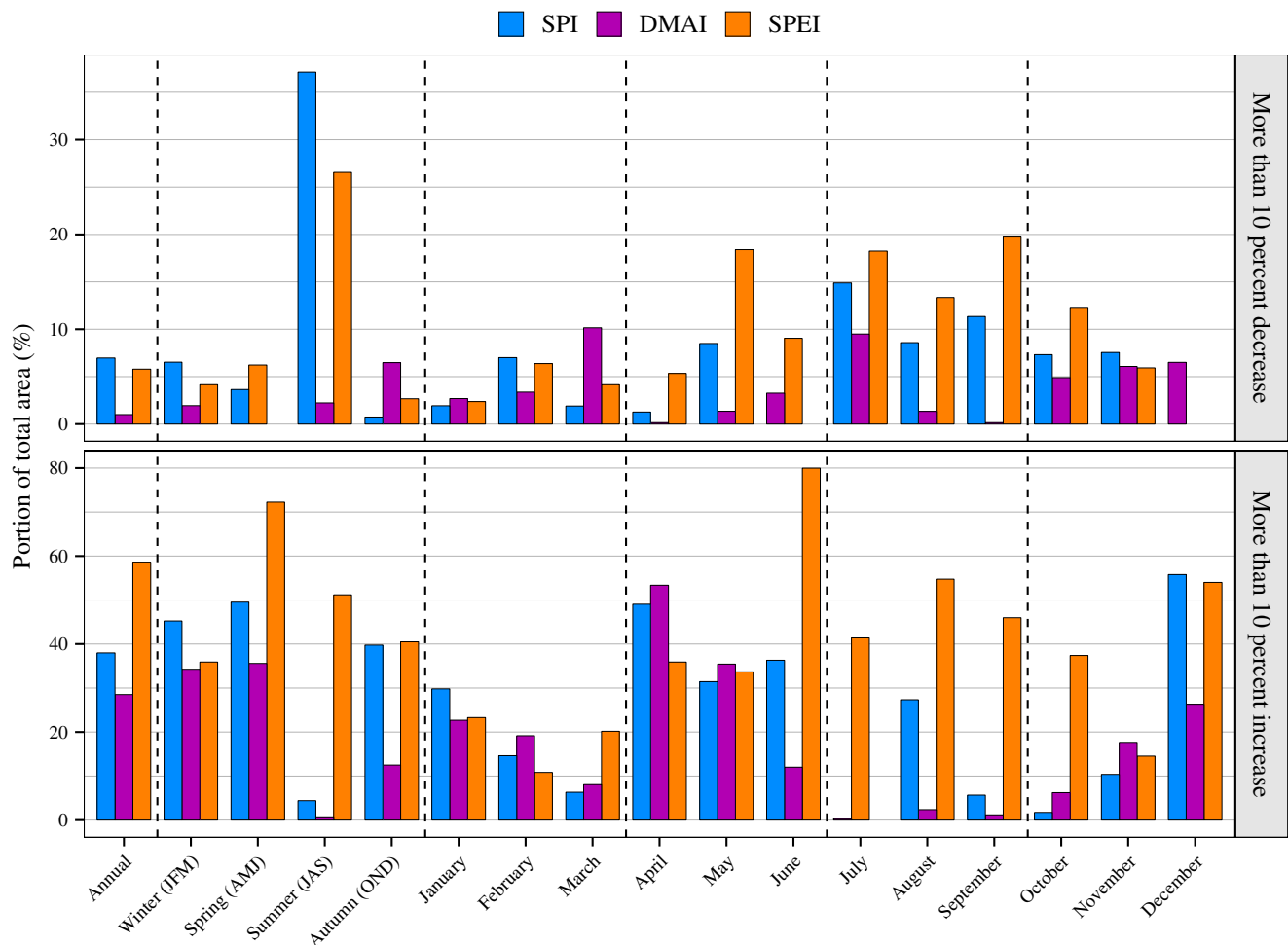
Fig. 11 Portion of the grid cells where the frequency of moderate to severe (M–S) droughts over 1987–2016 has increased/decreased by at least by 10% as compared with the period 1957–1986, according to the SPI, DMAI, and SPEI. For the thresholds used to define M–S droughts, please refer to Table 1

precipitation and increase in temperature and potential evapotranspiration, it seems necessary for farmers and policy-makers to adopt appropriate measures in response to recent climate changes. Improved planting scheme and adoption of more resilient genotypes, application of supplementary irrigation (Ramezani Etedali et al. 2013), and more efficient irrigation systems (Ababaei and Ramezani Etedali 2016) along with changing sowing dates could be among the adaptation strategies.

In Iran, most winter crops are planted in November (Ramezani Etedali et al. 2016; Ramezani Etedali et al. 2013). Adoption of earlier sowing dates can lead to the coincidence of the most sensitive early growth stages with increased precipitation in November. Over the last three decades, November has been the only month in which drought indexes (and precipitation) are shown to have increased. On the other hand, earlier sowing helps crops avoid terminal drought and heat waves over the warmer months of spring and early summer, which were shown to have experienced decreasing trends in all drought indexes.

The results of this study show that the monthly time series of the CRU TS 4.01 dataset, which has an almost complete spatial and temporal coverage in Iran over the last 60 years, are promising alternatives to weather station observations, especially in data-scarce regions of the country. Moreover, we conclude that it is not sufficient to assess the temporal and spatial variation of drought using just one drought/aridity index as different indexes carry different information and must be evaluated together to present a better picture of the impacts of the changing climate. The optimal choice of the aridity and/or drought indexes depends on the objectives of the study and the availability of data. The SPEI index proved to be an appropriate choice, especially when it comes to investigating the spatiotemporal variations of agricultural drought, as it considers precipitation and potential transpiration, the source and demand terms of the water balance equation. Analysis of variations at the seasonal and monthly scales helps better understand the recent climate change and target the most crucial features of it when it comes to formulating adaptation strategies.

References

Ababaei B, Ramezani Etedali H (2016) Water footprint assessment of main cereals in Iran. Agric Water Manag 179:401–411. https://doi.org/10.1016/j.agwat.2016.07.016

Ababaei B, Sohrabi T, Mirzaei F (2014) Development and application of a planning support system to assess strategies related to land and water resources for adaptation to climate change. Clim Risk Manag 6:39–50. https://doi.org/10.1016/j.crm.2014.11.001

Afshari Azad M, Shabanzadeh F (2010) A study of trend of wind speed changes in Rasht Synoptic Meteorological Station. [in Persian]

Ahmadi H, Fallahghalhary G, Shaemi A (2016) Estimating and evaluating the trends of annual reference evapotranspiration based on influential climatic parameters in the north east of Iran. [in Persian]. Iranian J Water and Soil Sci 25:257–269

Ahmadi F, Nazeri Tahroudi M, Mirabbasi R, Khalili K, Jhajharia D (2018) Spatiotemporal trend and abrupt change analysis of temperature in Iran. Meteorol Appl 25:314–321. https://doi.org/10.1002/met.1694

Allen RG, Pereira LS, Raes D, Smith M (1998) Crop evapotranspiration - guidelines for computing crop water requirements - FAO irrigation and drainage paper 56, Irrigation and Drainage

Araghi A, Martinez CJ, Adamowski J, Olesen JE (2018) Spatiotemporal variations of aridity in Iran using high-resolution gridded data. Int J Climatol 38:2701–2717. https://doi.org/10.1002/joc.5454

Azim NH, Subki A, Yusof ZNB (2018) Abiotic stresses induce total phenolic, total flavonoid and antioxidant properties in Malaysian indigenous microalgae and cyanobacterium. Malaysian J Microbiol 14:25–33. https://doi.org/10.1017/CBO9781107415324.004

Baltas E (2007) Spatial distribution of climatic indices in northern Greece. Meteorol Appl 14:69–78. https://doi.org/10.1002/met.7

Barnett TP, Pierce DW, Hidalgo HG, Bonfils C, Santer BD, Das T, Bala G, Wood AW, Nozawa T, Mirin AA, Cayan DR, Dettinger MD (2008) Human-induced changes in the hydrology of the Western United States. Science 319:1080–1083. https://doi.org/10.1126/science.1152538

Bazrafshan J (2017) Effect of air temperature on historical trend of long-term droughts in different climates of Iran. Water Resour Manag 31:4683–4698. https://doi.org/10.1007/s11269-017-1773-8

Bronaugh D, Werner A (2015) Package 'zyp.' R Cran

Davy R, Esau I, Chernokulsky A, Outten S, Zilitinkevich S (2017) Diurnal asymmetry to the observed global warming. Int J Climatol 37:79–93. https://doi.org/10.1002/joc.4688

Deniz A, Toros H, Incecik S (2011) Spatial variations of climate indices in Turkey. Int J Climatol 31:394–403. https://doi.org/10.1002/joc.2081

Dinpazhooh Y (2010) Analysis of trends in reference evapotranspiration in Zabol. [in Persian]. Nivar 70, 23–34

Eini MR, Javadi S, Delavar M (2018) Evaluating the performance of CRU and NCEP CFSR global reanalysis climate datasets, in hydrological simulation by SWAT model (case study: Maharlu Basin). Iran Water Resour Res 14:32–44

Elsner MM, Cuo L, Voisin N, Deems JS, Hamlet AF, Vano JA, Mickelson KEB, Lee S-Y, Lettenmaier DP (2010) Implications of 21st century climate change for the hydrology of Washington state. Clim Chang 102:225–260. https://doi.org/10.1007/s10584-010-9855-0

Fontaine MM, Steinemann AC (2009) Assessing vulnerability to natural hazards: impact-based method and application to drought in Washington state. Nat Hazards Rev 10:11–18. https://doi.org/10.1061/(ASCE)1527-6988(2009)10:1(11)

Ghahraman N, Gharakhani A (2010) Trend analysis of mean wind speed in different climatic regions of Iran. [in Persian]

Ghasemi AR (2015) Changes and trends in maximum, minimum and mean temperature series in Iran. Atmos Sci Lett 16:366–372. https://doi.org/10.1002/asl2.569

Gibbs W, Maher JV (1967) Rainfall deciles as drought indicators. Bureau of Meteorology, Melbourne

Giorgi F, Francisco R (2000) Evaluating uncertainties in the prediction of regional climate change. Geophys Res Lett 27:1295–1298. https://doi.org/10.1029/1999GL011016

Golian S, Mazdiyasni O, AghaKouchak A (2015) Trends in meteorological and agricultural droughts in Iran. Theor Appl Climatol 119:679–688. https://doi.org/10.1007/s00704-014-1139-6

Gu G, Adler RF (2015) Spatial patterns of global precipitation change and variability during 1901−2010. J Clim 28:4431–4453. https://doi.org/10.1175/JCLI-D-14-00201.1

Guttman NB (1998) Comparing the Palmer Drought Index and The Standardized Precipitation Index. J Am Water Resour Assoc 34:113–121. https://doi.org/10.1111/j.1752-1688.1998.tb05964.x

Hajihoseini H, Hajihoseini M, Najafi A, Morid S, Delavar M (2015) Assessment of changes in hydro-meteorological variables upstream of Helmand Basin during the last century using CRU data and SWAT model. Iran Water Resour Res 2 10, 38–52

Harris I, Jones PD, Osborn TJ, Lister DH (2014) Updated high-resolution grids of monthly climatic observations - the CRU TS3.10 dataset. Int J Climatol 34:623–642. https://doi.org/10.1002/joc.3711

Hosseinzadeh Talaee P, Shifteh Some'e B, Sobhan Ardakani S (2013) Time trend and change point of reference evapotranspiration over Iran. Theor Appl Climatol 116:639–647. https://doi.org/10.1007/s00704-013-0978-x

Hundecha Y, Bárdossy A (2005) Trends in daily precipitation and temperature extremes across western Germany in the second half of the 20th century. Int J Climatol 25:1189–1202. https://doi.org/10.1002/joc.1182

IPCC (2013) Summary for Policymakers. Climate Change 2013: The physical science basis. Contribution of Working Group I to the Fifth Assessment Report of the Intergovernmental Panel on Climate Change 33. https://doi.org/10.1017/CBO9781107415324

Irannezhad M, Marttila H, Kløve B (2014) Long-term variations and trends in precipitation in Finland. Int J Climatol 34:3139–3153. https://doi.org/10.1002/joc.3902

Karamouz M, Nazif S, Falahi M (2012) Hydrology and hydroclimatology. https://doi.org/10.1201/b13771

Kendall M, Gibbons JD (1990) Rank correlation methods, Science Forum

Khalili K, Tahoudi MN, Mirabbasi R, Ahmadi F (2016) Investigation of spatial and temporal variability of precipitation in Iran over the last half century. Stoch Env Res Risk A 30:1205–1221. https://doi.org/10.1007/s00477-015-1095-4

Lott N, Ross T (2005) Tracking and Evaluating U.S. Billion Dollar Weather Disasters, 1980-2005. NOAA's National Climatic Data Center 6

Madani K (2014) Water management in Iran: what is causing the looming crisis? J Environ Stud Sci 4:315–328. https://doi.org/10.1007/s13412-014-0182-z

Mahajan DR, Dodamani BM (2015) Trend analysis of drought events over upper Krishna Basin in Maharashtra. Aquat Procedia 4:1250–1257. https://doi.org/10.1016/j.aqpro.2015.02.163

Martonne E (1920) Géographie Physique (Physical Geography), 3rd edition. Librairie Armand Colin, Paris

Mckee TB, Doesken NJ, Kleist J (1993) The relationship of drought frequency and duration to time scales. AMS 8th Conference on Applied Climatology 179–184. citeulike-article-id:10490403

Miri M, Azizi G, Khoshakhlagh F, Ramimi M (2016) Evaluation statistically of temperature and precipitation datasets with observed data in Iran. Iranian J Watershed Management Sci Eng 10:40–50

Mitchell TD, Jones PD (2005) An improved method of constructing a database of monthly climate observations and associated high-

resolution grids. Int J Climatol 25:693–712. https://doi.org/10.1002/joc.1181

Mojtabavi SA, Shokoohi A, Ramezani Etedali H, Singh V (2018) Using regional virtual water trade and water footprint accounting for optimizing crop patterns to mitigate water crises in dry regions. Irrig Drain 67:295–305. https://doi.org/10.1002/ird.2170

Moral FJ, Paniagua LL, Rebollo FJ, García-Martín A (2017) Spatial analysis of the annual and seasonal aridity trends in Extremadura, southwestern Spain. Theor Appl Climatol 130:917–932. https://doi.org/10.1007/s00704-016-1939-y

Morid S, Smakhtin V, Moghaddasi M (2006) Comparison of seven meteorological indices for drought monitoring in Iran. Int J Climatol 26:971–985. https://doi.org/10.1002/joc.1264

Mote PW, Hamlet AF, Clark MP, Lettenmaier DP (2005) Declining mountain snowpack in western North America. Bull Am Meteorol Soc 86:39–49. https://doi.org/10.1175/BAMS-86-1-39

New M, Hulme M, Jones P (1999) Representing twentieth-century space-time climate variability. Part I: development of a 1961–90 mean monthly terrestrial climatology. J Clim. https://doi.org/10.1175/1520-0442(1999)012<0829:RTCSTC>2.0.CO;2

New M, Hulme M, Jones P (2000) Representing twentieth-century space-time climate variability. Part II: development of 1901-96 monthly grids of terrestrial surface climate. J Clim 13:2217–2238. https://doi.org/10.1175/1520-0442(2000)013<2217:RTCSTC>2.0.CO;2

Palmer WC (1965) Meteorological drought. U.S. weather bureau, res. Pap. No. 45

Parsafar N, Sabziparvar AA, Aeini A (2012) Evaluation of sensitivity of FAO-56 Penman-Monteith to the wind speed variations in Western Iran. [in Persian]

Pereira LS, Allen RG, Smith M, Raes D (2015) Crop evapotranspiration estimation with FAO56: past and future. Agric Water Manag 147:4–20. https://doi.org/10.1016/j.agwat.2014.07.031

Qian W, Hu Q, Zhu Y, Lee DK (2003) Centennial-scale dry-wet variations in East Asia. Clim Dyn 21:77–89. https://doi.org/10.1007/s00382-003-0319-3

Rahimzadeh F, Pedram M (2011) Reduction of wind power due to long term variation of wind speed in Esfehan province. [in Persian]. Nivar 13–22

Rajabi A, Shabanlou S (2012) Climate index changes in future by using SDSM in Kermanshah, Iran. J Env Res Dev 7:37–44

Ramezani Etedali H, Liaghat A, Parsinejad M, Tavakkoli AR, Bozorg Haddad O, Ramezani Etedali M (2013) Water allocation optimization for supplementary irrigation in rainfed lands to increase total income case study: upstream Karkheh River Basin. Irrig Drain 62:74–83. https://doi.org/10.1002/ird.1700

Ramezani Etedali H, Liaghat A, Parsinejad M, Tavakkoli A (2016) AquaCrop model calibration and evaluation in irrigation management. Iranian J Irrig Drain 10:389–397

Ramezani Etedali H, Ababaei B, Kaviani A (2018) Analysis of long-term impact of climate change on temperature over Iran using the CRU dataset. Iranian J Water Soil Resour Conserv 8:25–48

Rana G, Katerji N (1998) A measurement based sensitivity analysis of the Penman-Monteith actual evapotranspiration model for crops of different height and in contrasting water status. Theor Appl Climatol 60:141–149. https://doi.org/10.1007/s007040050039

Raziei T, Arasteh PD, Saghfian B (2005) Annual rainfall trend in arid and semi-arid regions of Iran. ICID 21st European Regional Conference 1–8

Raziei T, Saghafian B, Paulo AA, Pereira LS, Bordi I (2009) Spatial patterns and temporal variability of drought in Western Iran. Water Resour Manag 23:439–455. https://doi.org/10.1007/s11269-008-9282-4

Raziei T, Mofidi A, Santos JA, Bordi I (2012) Spatial patterns and regimes of daily precipitation in Iran in relation to large-scale atmospheric circulation. Int J Climatol 32:1226–1237. https://doi.org/10.1002/joc.2347

Raziei T, Daryabari J, Bordi I, Pereira LS (2014) Spatial patterns and temporal trends of precipitation in Iran. Theor Appl Climatol 115:531–540. https://doi.org/10.1007/s00704-013-0919-8

Rezayi Banafsheh M, Javan K, Zainali B (2011) Trend analysis of wind speed in the north west of Iran. [in Persian]

Robock A, Vinnikov KY, Srinivasan G, Entin JK, Hollinger SE, Speranskaya NA, Liu S, Namkhai A, Robock A, Vinnikov KY, Srinivasan G, Entin JK, Hollinger SE, Speranskaya NA, Liu S, Namkhai A (2000) The global soil moisture data bank. Bull Am Meteorol Soc 81:1281–1299. https://doi.org/10.1175/1520-0477(2000)081<1281:TGSMDB>2.3.CO;2

Saboohi R, Soltani S, Khodagholi M (2012) Trend analysis of temperature parameters in Iran. Theor Appl Climatol 109:529–547. https://doi.org/10.1007/s00704-012-0590-5

Shafer BA, Dezman LE (1982) Development of a surface water supply index (SWSI) to assess the severity of drought conditions in snowpack runoff areas. Proceedings of the 50th Annual Western Snow Conference

Shelton ML (2009) Hydroclimatology: perspectives and applications. Cambridge University Press

Shukla S, Steinemann AC, Lettenmaier DP, Shukla S, Steinemann AC, Lettenmaier DP (2011) Drought monitoring for Washington state: indicators and applications. J Hydrometeorol 12:66–83. https://doi.org/10.1175/2010JHM1307.1

Tabari H, Aghajanloo MB (2013) Temporal pattern of aridity index in Iran with considering precipitation and evapotranspiration trends. Int J Climatol 33:396–409. https://doi.org/10.1002/joc.3432

Tabari H, Hosseinzadeh Talaee P (2011) Temporal variability of precipitation over Iran: 1966-2005. J Hydrol 396:313–320. https://doi.org/10.1016/j.jhydrol.2010.11.034

Tabari H, Talaee PH, Ezani A, Some'e BS (2012) Shift changes and monotonic trends in autocorrelated temperature series over Iran. Theor Appl Climatol 109:95–108. https://doi.org/10.1007/s00704-011-0568-8

Tan C, Yang J, Li M (2015) Temporal-spatial variation of drought indicated by SPI and SPEI in Ningxia Hui autonomous region, China. Atmosphere 6:1399–1421. https://doi.org/10.3390/atmos6101399

Vicente-Serrano SM, Beguería S, López-Moreno JI (2010) A multiscalar drought index sensitive to global warming: the standardized precipitation evapotranspiration index. J Clim 23:1696–1718. https://doi.org/10.1175/2009JCLI2909.1

Wang A, Lettenmaier DP, Sheffield J (2011) Soil moisture drought in China, 1950-2006. J Clim 24:3257–3271. https://doi.org/10.1175/2011JCLI3733.1

Wilks DS (20060 Statistical methods in the atmospheric sciences, Methods Elsevier/Academic Press https://doi.org/10.1016/B978-0-12-385022-5.00018-X

Wu H, Hayes MJ, Weiss A, Hu Q (2001) An evaluation of the Standardized Precipitation ndex, the China-Z Index and the statistical Z-Score. Int J Climatol 21:745–758. https://doi.org/10.1002/joc.658

Xin X, Yu R, Zhou T, Wang B (2006) Drought in late spring of South China in recent decades. J Clim 19:3197–3206. https://doi.org/10.1175/JCLI3794.1

Yang H, Yang D (2012) Climatic factors influencing changing pan evaporation across China from 1961 to 2001. J Hydrol 414–415:184–193. https://doi.org/10.1016/j.jhydrol.2011.10.043

Yue S, Pilon P, Phinney B, Cavadias G (2002) The influence of autocorrelation on the ability to detect trend in hydrological series. Hydrol Process 16:1807–1829. https://doi.org/10.1002/hyp.1095

Zhai J, Su B, Krysanova V, Vetter T, Gao C, Jiang T (2010) Spatial variation and trends in PDSI and SPI indices and their relation to streamflow in 10 large regions of China. J Clim 23:649–663. https://doi.org/10.1175/2009JCLI2968.1

Zhang Y, Cai W, Chen Q, Yao Y, Liu K (2015) Analysis of changes in precipitation and drought in Aksu River Basin, Northwest China. Adv Meteorol 2015:1–15. https://doi.org/10.1155/2015/215840

Zolfaghari H, Masoompour J, Yeganefar M, Akbary M (2016) Studying spatial and temporal changes of aridity in Iran. Arab J Geosci 9. https://doi.org/10.1007/s12517-016-2379-9

Zou X, Zhai P, Zhang Q (2005) Variations in droughts over China: 1951-2003. Geophys Res Lett 32:1–4. https://doi.org/10.1029/2004GL021853